Solving Embedded Crack Problems Using the Numerical Green's Function and a meshless Coupling Procedure: Improved Numerical Integration

E.F. Fontes Jr[1], J.A.F. Santiago[1] and J.C.F. Telles[1]

Abstract: An iterative coupling procedure using different meshless methods is presented to solve linear elastic fracture mechanic (LEFM) problems. The domain of the problem is decomposed into two sub-domains, where each one is addressed using an appropriate meshless method. The method of fundamental solutions (MFS) based on the numerical Green's function (NGF) procedure to generate the fundamental solution has been chosen for modeling embedded cracks in the elastic medium and the meshless local Petrov-Galerkin (MLPG) method has been chosen for modeling the remaining sub-domain. Each meshless method runs independently, coupled with an iterative update of interface variables to achieve the final convergence. The coupling procedure is easy to apply for any LEFM problems with one or more cracks and can save time in the construction of the problem representation by points. In addition, different numerical integral approaches are tested for to compute integrals of the MLPG method.

The iterative solution procedure presented yields good results as compared with the boundary element method and alternative solutions for stress intensity factor computations.

Keywords: meshless, MFS, MLPG, crack, NGF, iterative coupling.

1   Introduction

Modeling of computational mechanics problems by meshless methods is increasingly attracting the attention of the research community and in many cases is proving to be a viable alternative to mesh type methods, like the boundary element method (BEM) and the finite element method (FEM). Different types of meshless methods can be found in the works by Atluri and Zhu (1998) and Nguyen, Rabczuk, Bordas, and Duflot (2008). Interesting coupling procedures between

---

[1] Civil Engineering Programme, COPPE, UFRJ, RJ, Brazil.

meshless methods can be adopted, improving not only efficiency, but also solution accuracy for different coupled engineering problems as shown in the works by Gu and Zhang (2008) and Godinho and Soares Jr. (2013).

Truly meshless methods based on integral equations such as the meshless local Petrov-Galerkin (MLPG) method by Atluri and Zhu (1998) and the method finite spheres by De and Bathe (2001) include domain integrals with complicated non polynomial integrands due to the intrinsic characteristics of their shape functions. By using conventional Gaussian quadrature, these methods may need excessive integration points to achieve acceptable accuracy, increasing computational costs. Alternative procedures to deal with this drawback use newly developed quadrature or cubature rules to perform numerical integration in a more efficient fashion, as seen in the works by De and Bathe (2001), Pecher (2006), Mazzia, Ferronato, Pini, and Gambolati (2007) and Mazzia and Pini (2010). Here, an integration method is proposed for the MLPG-1, it derives from a generalized Gaussian quadrature rule, based on a wider class of functions, as presented in Ma, Rokhlin, and Wandzura (1996). In the work presented in Jayan and Nagaraja (2011), a generalized Gaussian quadrature rule is used to compute numerical integrations over two-dimensional domains, comprised of linear sides, for applications in FEM. In here, such a generalized Gaussian quadrature rule is adopted and modified for quadratures over 2D circles, based on Fubini's [Thomas and Finney (1996)] theorem.

In addition to the proposed quadrature process, the present work also introduces an efficient iterative coupling routine to solve linear elastic fracture mechanics (LEFM) problems. Here, the iterative coupling between the method of fundamental solutions (MFS) and the MLPG method is considered. The problem domain is divided in sub-domains. The MFS is adopted for modeling regions with embedded cracks like in Fontes Jr., Santiago, and Telles (2013) while for standard elastic regular sub-domains the MLPG is selected. In order to construct the solution, the MFS, firstly developed by Kupradze and Aleksidze (1964), uses only a superposition of fundamental solutions associated to the problem. In the case of LEFM problems one can use the numerical Green's function (NGF) procedure developed by Telles, Castor, and Guimaraes (1995) and Castor and Telles (2000); Guimaraes and Telles (2000). The concept of NGF was successfully extended to the meshless context generating very good results in the works by Miers and Telles (2006); Fontes Jr., Santiago, and Telles (2013). This strategy permits to solve the principal problem in a decoupled manner, without need to introduce a large number of near crack tip points, to capture accurate stress intensity factors (SIF), as opposed to the standard MLPG approach for fracture mechanics applications found in the works by Gu and Zhang (2008) and Ching and Batra (2001). Finally, a comparison between different Gaussian quadrature rules is also included when solving LEFM problems with the

proposed iterative coupling procedure. A similar iterative coupling idea, however in a mesh-type context, is the alternating/coupling procedure between FEM and the symetric Galerkin BEM (SGBEM) developed by Han and Atluri (2002) to solve fracture and fatigue analyses of various engineering structures.

This text is organized as follows: first the generalized Gaussian quadrature rule is presented and the numerical meshless methods are briefly introduced. The iterative coupling procedure is then detailed. Finally we show two examples of problems solved by using the developed iterative coupling and different quadrature rules to illustrate the degree of approximation found for stress intensity factors.

2 Numerical integration

A comparison of different numerical integration rules has been presented in the article by Mazzia, Ferronato, Pini, and Gambolati (2007) and shows that the integration rule that applies one-dimensional Gauss-Legendre for radial-integration and midpoint rule for angular-integration, introduced by De and Bathe (2001) and Pierce (1957), here denominated rule 2, gives better results for circles in the MLPG-1 method. The traditional Gaussian quadrature rule used in the work by Atluri and Zhu (1998) has been denoted here as rule 1.

In what follows the coordinate transformation used to perform the generalized Gaussian quadrature, here proposed, is described.

2.1 Generalized Gaussian quadrature

The integral of an arbitrary function, $f(x,y)$, over a two dimensional domain, according to the hypothesis of Fubini's theorem, is given by,

$$\iint_{\Omega} f(x,y)d\Omega = \int_a^b \int_{r(x)}^{s(x)} f(x,y)dydx$$

$$(1)$$

$$= \int_a^b \int_{r(y)}^{s(y)} f(x,y)dxdy$$

Applying Eq. (1) for a two-dimensional circle centered at the origin of a domain Ω_s with radius r_0 one has

$$\iint_{\Omega_s} f(x,y)d\Omega = \int_{-r_0}^{r_0} \int_{-\sqrt{r_0^2-x^2}}^{\sqrt{r_0^2-x^2}} f(x,y)dydx \qquad (2)$$

The integral in Eq. (2) can be transformed to a local coordinate system by the following coordinate transformation

$$x = x(\xi, \eta) = r_0 \xi \tag{3}$$

$$y = y(\xi, \eta) = \sqrt{1 - \xi^2} \, r_0 \eta. \tag{4}$$

where $-1 \le \xi, \eta \le +1$. The determinant of the Jacobian is therefore:

$$|\mathbf{J}| = \frac{\partial x}{\partial \xi} \frac{\partial y}{\partial \eta} - \frac{\partial x}{\partial \eta} \frac{\partial y}{\partial \xi} = \sqrt{1 - \xi^2} \, r_0^2 \tag{5}$$

Applying Eqs. (3-5) to Eq. (2), the integral can be written in the new coordinate system as:

$$\int_{-r_0}^{r_0} \int_{-\sqrt{r_0^2 - x^2}}^{\sqrt{r_0^2 - x^2}} f(x, y) dy dx = \int_{-1}^{1} \int_{-1}^{1} f(x(\xi, \eta), y(\xi, \eta)) \, |\mathbf{J}| \, d\eta \, d\xi \tag{6}$$

Hence, the numerical integration of Eq. (6) can be performed by applying Gaussian quadrature rules

$$\int_{-1}^{1} \int_{-1}^{1} f(x(\xi, \eta), y(\xi, \eta)) |\mathbf{J}| d\eta d\xi = \sum_{i=1}^{N} \sum_{j=1}^{N} \tau_i \tau_j |\mathbf{J}|_i f(x(\xi_i, \eta_j), y(\xi_i, \eta_j)) \tag{7}$$

where N is the integration order, ξ_i and η_j are integration points. The generalized Gaussian integration in Eq. (7) is the one denoted here as rule 3. The Gauss-Jacobi quadrature rule is the one employed, using $\omega(x) = (1-x)^\gamma (1+x)^\zeta$ as a weight function. When $\gamma = \zeta = 0$ one gets the Gauss-Legendre integration weights $\tau_i = \omega_i$ and $\tau_j = \omega_j$.

The integration points distribution for the integration rules compared here can be seen in Fig. 1. Using the abscissa of the Gauss-Jacobi formula with $\gamma = \zeta = 0$ in rule 3, one gets the integration points distribution of Fig. 1(c). A wider class of functions can also be used with Eq. (7) as seen in Ma, Rokhlin, and Wandzura (1996), depending on the characteristics of the integrand on the interval $[-1, 1]$.

3   Meshless methods

3.1   *Governing equations*

LEFM problems are formulated based on the linear elasticity theory. For a two-dimensional linear elastic body Ω, bounded by the boundary Γ, the well-known

Navier equation in terms of displacements u_i (generalized i directions displacements) can be written in the form:

$$Gu_{j,kk} + \frac{G}{1-2v}u_{k,kj} + b_j = 0 \tag{8}$$

where G is the shear modulus, v is the Poisson's ratio and b_j is the body force components. The displacement u_i is solved from Eq. (8) satisfying the boundary conditions:

$$\begin{aligned} u_i &= \bar{u}_i, \quad \text{on } \Gamma_u \\ p_i &= \sigma_{ji}n_j = \bar{p}_i, \quad \text{on } \Gamma_p \end{aligned} \tag{9}$$

In the above equation, $\bar{u}_i$ and $\bar{p}_i$ are the prescribed displacements and tractions on the boundary Γ_u and Γ_p, respectively. The external boundary of the body is $\Gamma = \Gamma_u \cup \Gamma_p$.

3.2 Meshless local Petrov-Galerkin

The so-called truly meshless denomination stands for a class of meshless methods, such as MLPG, that do not require any kind of element or mesh to generate approximations for the field variables or even cells to perform numerical integrals, e.g. see Atluri and Zhu (1998). The numerical integrals are performed on local sub-domains, covering the complete global domain, and the field variables are approximated by an appropriate interpolation scheme. Here, circles are used to represent local sub-domains Ω_s and whose respective radius r_0 is defined as:

$$r_0 = \alpha l_1 \tag{10}$$

where α is a scale factor and l_1 is the value in the first position of vector $\mathbf{l}$. Vector $\mathbf{l}$ is ordered incrementally according to the distance values of point $\mathbf{x}$ and its neighborhood points.

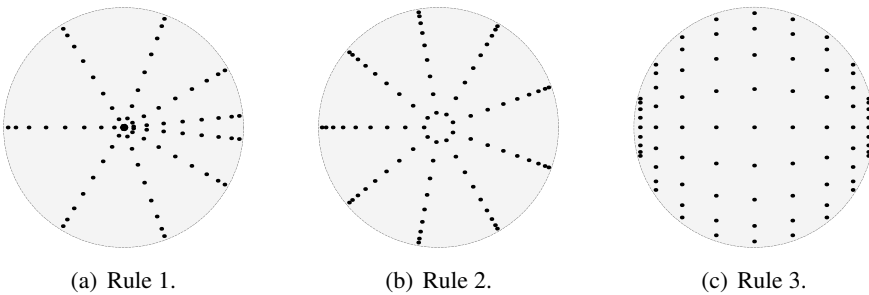(a) Rule 1. (b) Rule 2. (c) Rule 3.

Figure 1: Positions of integration points in each numerical integration approach.

Among several formulations of the MLPG method, here one has used the version known as MLPG-1, as described in Atluri and Zhu (2000), with the displacement field **u** approximated by the moving least square (MLS) interpolation, see Lancaster and Salkauskas (1981).

Given a set of points in the neighborhood of point **x**, an approximation function can be constructed and the field variable **u**(**x**) can be approximated by:

$$\mathbf{u}(\mathbf{x}) = \Phi^{\mathrm{T}}(\mathbf{x})\,\mathbf{u}_j^{\mathrm{PG}} \tag{11}$$

where $\Phi^{\mathrm{T}}(\mathbf{x})$ comes from the MLS approximation and needs to be carried out for each point **x** within the local sub-domain using a compact support to ensure locally approximated functions. The superscript PG is included to indicate MLPG variables. The domain of definition of the MLS is a circle of radius r_i defined by:

$$r_i = \beta\, l_{O(m)} \tag{12}$$

where β is a scale factor and $l_{O(m)}$ is its distance value in the position $O(m)$ of vector **l**, depending on the polynomial order $O(m)$ approximation used by the MLS.

In the MLPG-1, the same weight function $w_i(\mathbf{x})$ of the MLS approximation selected to be the test function of the corresponding local sub-domain Ω_s over which integrals are to be calculated. Here, the following quartic spline function has been used:

$$w_i(\mathbf{x}) = \begin{cases} 1 - 6\left(\dfrac{d_i}{r}\right)^2 + 8\left(\dfrac{d_i}{r}\right)^3 - 3\left(\dfrac{d_i}{r}\right)^4, & 0 \le d_i \le r \\[2mm] 0, & d_i \ge r \end{cases} \tag{13}$$

where $d_i = \|\mathbf{x} - \mathbf{x}_i\|_2$ and r can either be the support radius r_i defined in Eq. (12) for MLS approximations or the radius r_0 defined in Eq. (10) for the test function.

As shown in Atluri and Zhu (2000), one can obtain a generalized local weak form of Eq. (8) and boundary conditions (9), over a local sub-domain $\Omega_{\mathbf{s}}$, given by each point **x** and local boundary $\Gamma_{\mathbf{s}} = L_{\mathbf{s}} \cup \Gamma_{\mathbf{su}} \cup \Gamma_{\mathbf{st}}$. Bearing in mind that the local sub-domains are supposed to cover the whole global domain and taking into account the stress-strain and the strain-displacement relations, a system of linear equations can be written:

$$\mathbf{K}\mathbf{u}^{\mathrm{PG}} = \mathbf{f} \tag{14}$$

where, for $i, j = 1, 2, \cdots, n$

$$\mathbf{K}_{ij} = \int_{\Omega_s} \varepsilon_{\mathbf{w}_i} \mathbf{D}\mathbf{B}_j\, d\Omega + \mu \int_{\Gamma_{su}} \mathbf{w}_i(\mathbf{x})\Phi_j\, d\Gamma - \int_{\Gamma_{su}} \mathbf{w}_i(\mathbf{x})\mathbf{N}\mathbf{D}\mathbf{B}_j\, d\Gamma \tag{15}$$

$$\mathbf{f}_i = \int_{\Gamma_{st}} \mathbf{w}_i(\mathbf{x})\bar{\mathbf{p}}\,d\Gamma + \mu \int_{\Gamma_{su}} \mathbf{w}_i(\mathbf{x})\bar{\mathbf{u}}\,d\Gamma + \int_{\Omega_s} \mathbf{w}_i(\mathbf{x})\mathbf{b}\,d\Omega \tag{16}$$

where $\mathbf{D}$ is a matrix that depends on whether the problem is one of plane stress or plane strain, $\varepsilon_{\mathbf{w}_i}$ and $\mathbf{B}_j$ represent partial derivatives of the weight function $\mathbf{w}_i$ and of the shape function Φ_j, respectively, $\mathbf{N}$ is a matrix composed of terms related to the outward normal direction to the boundary and μ is a penalty factor employed to enforce satisfaction of the essential boundary conditions.

3.3   *Method of fundamental solutions*

The fundamental solution used in this work is the numerical Green's function (NGF) developed by Telles, Castor, and Guimaraes (1995). The Green's function is written in terms of a superposition of the Kelvin fundamental solution and a complementary part, which ensures that the final result is equivalent to an embedded crack, unloaded, within the infinite elastic medium subjected to a unit applied load, given by

$$u_{ij}^*(\xi,\chi) = u_{ij}^{\mathcal{K}}(\xi,\chi) + u_{ij}^{\mathcal{C}}(\xi,\chi) \tag{17}$$

$$p_{ij}^*(\xi,\chi) = p_{ij}^{\mathcal{K}}(\xi,\chi) + p_{ij}^{\mathcal{C}}(\xi,\chi) \tag{18}$$

where $u_{ij}^*(\xi,\chi)$ and $p_{ij}^*(\xi,\chi)$ are the fundamental displacements and tractions in j direction at the field point χ due to a unit point load applied at the source point ξ in i direction, respectively (Fig. 2). The kernels $u_{ij}^{\mathcal{K}}(\xi,\chi)$ and $p_{ij}^{\mathcal{K}}(\xi,\chi)$ represent the known Kelvin fundamental solution. Here, $u_{ij}^{\mathcal{C}}(\xi,\chi)$ and $p_{ij}^{\mathcal{C}}(\xi,\chi)$ stand for complementary components of the problem defined as an infinite space containing crack(s) of arbitrary geometry under applied distributed loads required to cancel the Kelvin's tractions as required by the original fundamental problem. For further details about the use of the NGF approach with the method of fundamental solutions (MFS), see Fontes Jr., Santiago, and Telles (2013).

Consider the boundary value problem of an elastic solid of domain Ω enclosed by a boundary Γ governed by the Navier Equation (8), subjected to mixed boundary conditions, as given in Eq. (9), in the absence of body forces. The MFS developed by Kupradze and Aleksidze (1964) establishes that the approximate solution can be constructed by a summation of similar problems solutions given by the following matrix notation

$$\mathbf{u}^{\text{FS}}(\chi) = \mathbf{G}\,\mathbf{d}(\xi) \tag{19}$$

$$\mathbf{p}^{\text{FS}}(\chi) = \mathbf{H}\,\mathbf{d}(\xi) \tag{20}$$

where $\mathbf{u}^{\text{FS}}$ and $\mathbf{p}^{\text{FS}}$ are approximations for displacements and tractions, corresponding to a point $\chi \in \Omega^{\text{FS}} \cup \Gamma^{\text{FS}}$, respectively. The coefficients of matrices $\mathbf{G}$ and $\mathbf{H}$ are
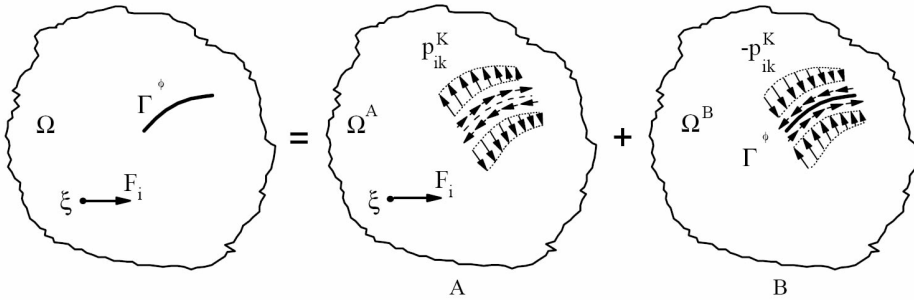
Figure 2: Green's function generated by the superposition of the physical states (A) and (B).
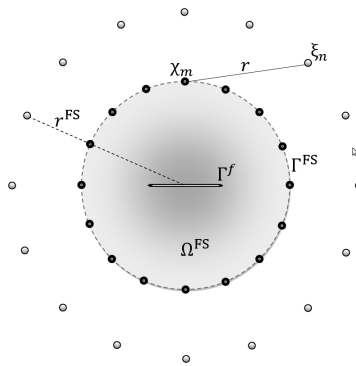

Figure 3: Overview of the MFS of a circular domain Ω^{FS} with a center crack. ξ_n are the source points and χ_m are the field points.

given by u_{ij}^* and p_{ij}^*, respectively. Usually $\xi_n \notin \Omega^{\text{FS}} \cup \Gamma^{\text{FS}}$ are the virtual sources and $\mathbf{d}(\xi)$ is the unknown weight vector. The superscript FS indicates MFS variables.

First, an indirect problem must be solved to compute the weighting parameters $\mathbf{d}(\xi)$. The boundary Γ is represented by M field points χ_m, then N source points ξ_n are chosen and distributed forming a fictitious boundary surrounding Γ^{FS} (see Figure 3). In order to enforce the boundary conditions (9) in Eqs. (19-20) a linear system of equations is generated.

$$\sum_{n=1}^{N} u_{ij}^*(\xi_n, \chi_m)\, d_i(\xi_n) = \bar{u}_j(\chi_m)\,, \qquad \chi_m \in \Gamma_u,\ m = 1, \cdots, M, \tag{21}$$

$$\sum_{n=1}^{N} p_{ij}^{*}(\xi_n, \chi_m) \, d_i(\xi_n) = \bar{p}_j(\chi_m), \qquad \chi_m \in \Gamma_p, \ m = 1, \cdots, M. \tag{22}$$

Applying either Eq. (21) or Eq. (22) for the M discrete field points x_m, the linear system of equations above can be written in matrix notation

$$\mathbf{A}\mathbf{d}(\xi) = \mathbf{b} \tag{23}$$

where $\mathbf{A}$ is a dense matrix of NGF coefficients, $\mathbf{d}$ the unknown weight vector, and $\mathbf{b}$ the right-hand side vector of boundary conditions. Finally, once all weight source values of $\mathbf{d}$ are determined, the displacements and the tractions at any point on the boundary can be evaluated using Eqs. (19-20). In addition, the displacement at any point inside the domain can be evaluated using Eq. (19) and the stress values at any point can be computed using the standard approximation given by the MFS.

Following the idea of the MFS, the stress intensity factors (SIF) can be easily calculated by the superposition of the generalized openings of the crack and the weighting parameters d_i as can be seen in Fontes Jr., Santiago, and Telles (2013).
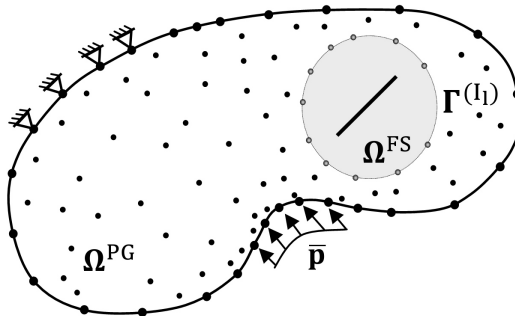

Figure 4: Overview of the iterative coupling procedure between the MFS-NGF and the MLPG to solve embedded crack problems.

4 The iterative coupling procedure

The goal of the iterative coupling to consider the global domain partitioned in sub-domains represented by different meshless methods and to enforce the coupling iteratively until a convergence criteria is satisfied. In this work the sub-domains are represented in the form of Fig. 4 and the sequential iterative algorithm proposed by Lin, Lawton, Caliendo, and Anderson (1996) has been adopted. The sub-domain Ω^{FS} comprehends a crack (or cracks) embedded and is dealt with the MFS-NGF, whereas sub-domain Ω^{PG} is to be solved by the MLPG method.

Considering the compatibility and equilibrium conditions at the common interface of the meshless methods:

$$\mathbf{u}_{\mathtt{I}_l}^{\mathtt{FS}} = \mathbf{u}_{\mathtt{I}_l}^{\mathtt{PG}} \tag{24}$$

$$\mathbf{p}_{\mathtt{I}_l}^{\mathtt{FS}} = -\mathbf{p}_{\mathtt{I}_l}^{\mathtt{PG}} \tag{25}$$

where the subscript $\mathtt{I}_l$ represents the common interface l and the vectors $\mathbf{u}^{\mathtt{FS}} = \left(\mathbf{u}_{FS}^{\mathtt{FS}} \ \mathbf{u}_{\mathtt{I}_l}^{\mathtt{FS}} \right)^{\mathtt{T}}, \mathbf{u}^{\mathtt{PG}} = \left(\mathbf{u}_{PG}^{\mathtt{PG}} \ \mathbf{u}_{\mathtt{I}_l}^{\mathtt{PG}} \right)^{\mathtt{T}}, \mathbf{p}^{\mathtt{FS}} = \left(\mathbf{p}_{FS}^{\mathtt{FS}} \ \mathbf{p}_{\mathtt{I}_l}^{\mathtt{FS}} \right)^{\mathtt{T}}$ and $\mathbf{p}^{\mathtt{PG}} = \left(\mathbf{p}_{PG}^{\mathtt{PG}} \ \mathbf{p}_{\mathtt{I}_l}^{\mathtt{PG}} \right)^{\mathtt{T}}$ represent the decomposed displacements and tractions for each meshless method.

The iterative coupling algorithm comes from a successive updating of the interface variables defined in Eqs. (24-25) as follow:

(i) The main problem is decomposed in two or more sub-problems and each one is modeled by either the MLPG method or the MFS when in the presence of cracks;

(ii) Choose over the common interface $\mathbf{u}_{\mathtt{I}_l}^{\mathtt{FS}} = \mathbf{0}$ for the MFS;

(iii) Solve Eq. (23) and obtain the tractions $\mathbf{p}_{\mathtt{I}_l}^{\mathtt{FS}}$ using Eq. (20) for sub-domain $\Omega^{\mathtt{FS}}$;

(iv) Assembly matrix and nodal force vector Eqs. (15-16) using $\mathbf{p}^{\mathtt{PG}} = \left[\mathbf{p}_{PG}^{\mathtt{PG}} - \mathbf{p}_{\mathtt{I}_l}^{\mathtt{FS}} \right]^{\mathtt{T}}$;

(v) Solve Eq. (14) for displacements $\mathbf{u}_{\mathtt{I}_l}^{\mathtt{PG}}$;

(vi) Check the convergence at interface values, i.e.

$$\frac{\left\| \mathbf{u}_{\mathtt{I}_l,n+1}^{\mathtt{FS}} - \mathbf{u}_{\mathtt{I}_l,n}^{\mathtt{FS}} \right\|}{\left\| \mathbf{u}_{\mathtt{I}_l,n+1}^{\mathtt{FS}} \right\|} \leq 10^{-6} \tag{26}$$

if yes then stop;

(vii) Otherwise set $\mathbf{u}_{\mathtt{I}_l,n+1}^{\mathtt{FS}} = (1-\lambda)\mathbf{u}_{\mathtt{I}_l,n}^{\mathtt{FS}} + \lambda \, \mathbf{u}_{\mathtt{I}_l,n}^{\mathtt{PG}}$, where λ is a relaxation parameter;

(viii) Return to step **iii** until convergence is achieved at step **vi**.

In all examples an optimal choice for the relaxation parameter λ as presented in Lin, Lawton, Caliendo, and Anderson (1996) has been used. Hence, considering the square error functional:

$$\mathscr{F}(\lambda) = \left\| \mathbf{u}_{\mathtt{I}_l,n+1}^{\mathtt{FS}}(\lambda) - \mathbf{u}_{\mathtt{I}_l,n}^{\mathtt{FS}}(\lambda) \right\|^2 \tag{27}$$

The minimization of Eq. (27) with respect to the relaxation parameter λ yields an optimal dynamic value for the next iteration as proved in Lin, Lawton, Caliendo, and Anderson (1996):

$$\lambda = \frac{\langle \mathbf{e}_n^{\text{FS}}, \mathbf{e}_n^{\text{FS}} - \mathbf{e}_n^{\text{PG}} \rangle}{\| \mathbf{e}_n^{\text{FS}} - \mathbf{e}_n^{\text{PG}} \|^2} \tag{28}$$

where $\mathbf{e}_n^{\text{FS}} = \mathbf{u}_{\text{I}_l,n}^{\text{FS}} - \mathbf{u}_{\text{I}_l,n-1}^{\text{FS}}$, $\mathbf{e}_n^{\text{PG}} = \mathbf{u}_{\text{I}_l,n}^{\text{PG}} - \mathbf{u}_{\text{I}_l,n-1}^{\text{PG}}$, $n > 1$ and $0 < \lambda \leq 1$.

5 Numerical results

Numerical results for iterative couplings between MFS-NGF and MLPG-1 methods, as applied to a dual crack interaction problem and a center crack problem, are presented. For all examples, the virtual sources have been distributed in a circular path way. The number of field points on the MFS has always been the same as the number of virtual sources. All results for the MLPG subdomains have been obtained using quadratic basis and quartic splines as the weight function, with circular compact supports.

5.1 Interaction between two cracks

The problem is an isotropic plate with two cracks, both of length $2a = 1.0$, subjected to a uniform stress (see Fig. 5(a)). This example was chosen to show an interesting capability of the iterative coupling procedure when using the NGF technique to represent the cracks. In Fig. 5(b) the circular sub-domains are modeled by the MFS-NGF procedure. The circular sub-domains for crack *AB* and crack *CD* have 18 and 14 points, respectively. Each crack is divided in 10 segments and each segment has 12 integration points.

For the MLPG sub-domain, 513 points have been used, the dimensions are $W = h = 10$, $2a/d = 0.1$, $\theta = 30^o$ and $\sigma = 1.0$. The numerical integrals in Eqs. (15-16) were carried out over local circles sub-domains by the traditional Gaussian quadrature, using 12×12 integration points for a subdomain Ω_s and 12 integration points for the boundaries Γ_{st} and Γ_{su}. Normalized SIF results are compared with BEM-NGF, for an infinite plate, in Tab. 1, to validate the coupled procedure.

Table 1: Normalized SIF for a plate with a/w=0.05 by the coupled procedure and an infinite plate by the BEM-NGF

	coupled procedure				BEM-NGF			
	Tip A	Tip B	Tip C	Tip D	Tip A	Tip B	Tip C	Tip D
K_{I}/K_0	1.0112	1.0112	0.7593	0.7591	1.0071	1.0072	0.7540	0.7546
K_{II}/K_0	-0.0007	-0.0008	0.4362	0.4365	-0.0005	-0.0006	0.4351	0.4351

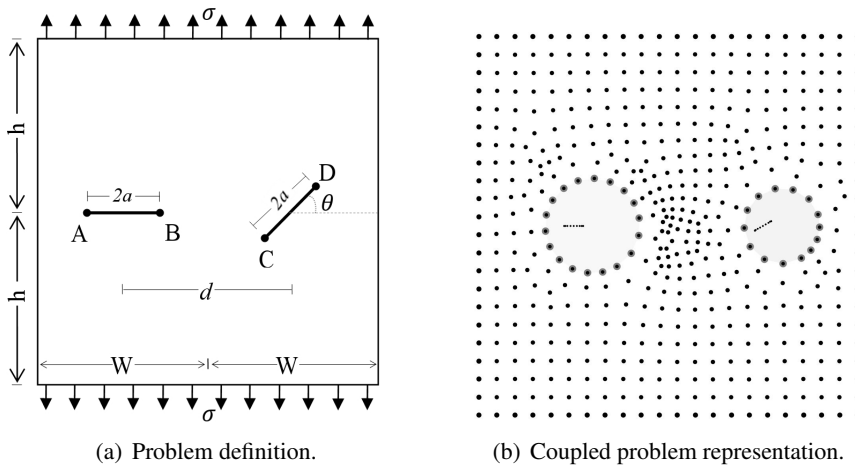(a) Problem definition.   (b) Coupled problem representation.

Figure 5: Dual cracks interaction problem.

5.2 Center crack

In this example the plate with a center crack problem of Fig. 6(a) is analyzed using the iterative coupling procedure. The Young's modulus used is $E = 2200.0$, Poisson ratio $v = 0.1$ and the applied traction $p = 1.0$. The plate dimensions are $W = 10$ and $L = 10$. In Fig. 6(a) the circular sub-domain is modeled by the MFS-NGF procedure using 32 points on the boundary. The MLPG sub-domain is represented by 285 points and the numerical integrals in Eqs. (15-16) have been carried out, on the local circle sub-domains, by the different integration techniques described in Subsection 2. It is worth mentioning that standard Gaussian quadrature concentrates integration points on the center of the integration domain (see Fig. 1(a)). Hence, traditional Gaussian quadrature gives better results when dealing with circular sub-domains that intersect the global boundary, as shown in Mazzia, Ferronato, Pini, and Gambolati (2007). Consequently, this procedure has always been used for circular sectors intersecting the global boundary. The different alternative rules, previously discussed, have been selected just for interior sub-domains.

Fig. 7 shows the relative error on the numerical SIF computation for each value of r^{FS}, in a logarithmic scale, in comparison with a closed form solution given by Snyder and Cruse (1975) for different numbers of quadrature points. As can be seen, rule 3 gives better results than rules 1 and 2 even for reduced numbers of gauss points (see Fig. 7(a)), when differences become more pronounced, generating reduced errors of less than 2% over almost the entire range of tested r^{FS} values considered, as seen in Figs. 7(a)-7(e).

The number of iterations of the coupling procedure is compared in Fig. 8 for each value of r^{FS} and different numbers of quadrature points. In Fig. 8(a), the iterative coupling procedure does not converge for 3×3 quadrature points when using rule 1 over most values of r^{FS}. As depicted in Figs. 8(a)-8(e), rule 3 still produces some advantages over rule 2 regarding the number of iterations required to obtain acceptable solutions.
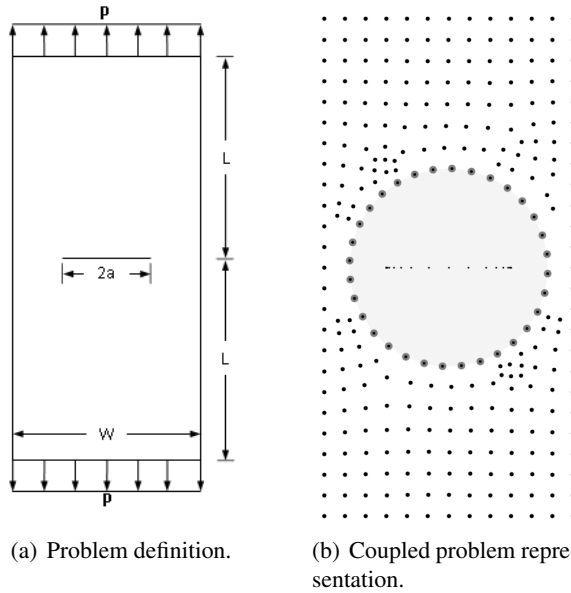

(a) Problem definition.

(b) Coupled problem repre-
sentation.

Figure 6: Plate with a center crack.

6   Concluding remarks

In this paper an iterative coupling between two meshless methods is presented to solve LEFM problems. The use of NGF in the MFS sub-domains allows for accurately solving crack problems saving computational cost. Good results for SIF computations were obtained in the examples presented. The generalized Gaussian quadrature presented shows efficiency for the coupling procedure and gives similar or even better results in comparison with the numerical integrations rules available in the literature for the last example considered. Further improvements can be obtained if one takes advantage of parallel computing, a natural procedure for the coupling routine presented here.
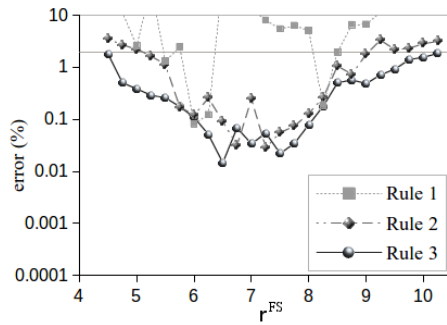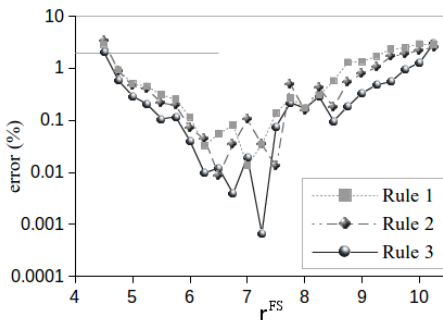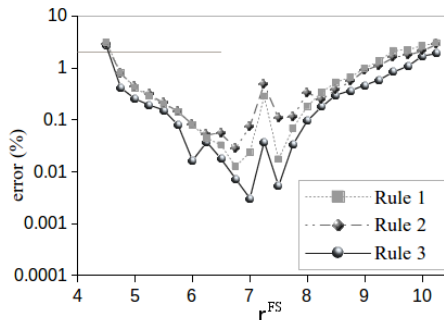
(a) 3x3 points.
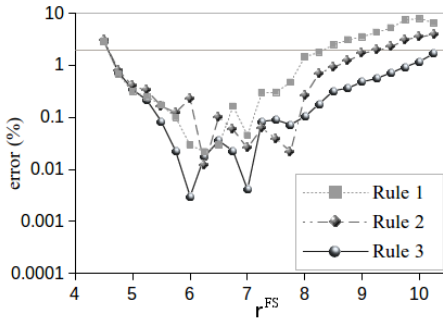
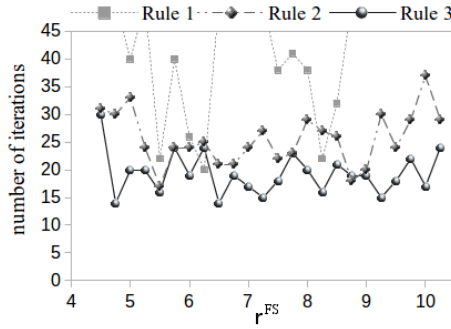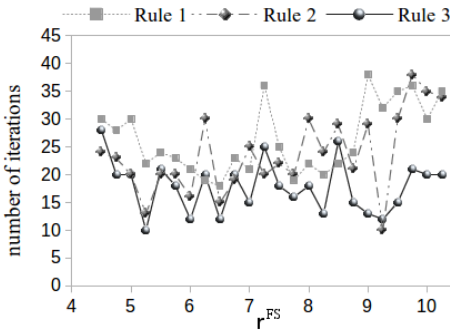(b) 4x4 points.
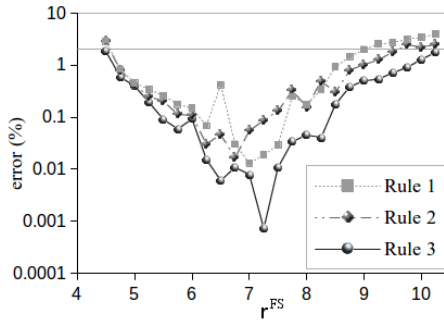
(c) 5x5 points.
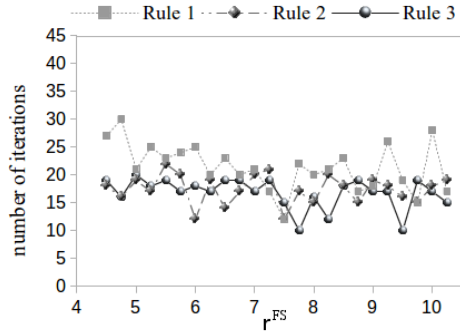

(d) 7x7 points.

(e) 9x9 points.

Figure 7: Relative error for the different number of Gauss points and r^{FS} values.
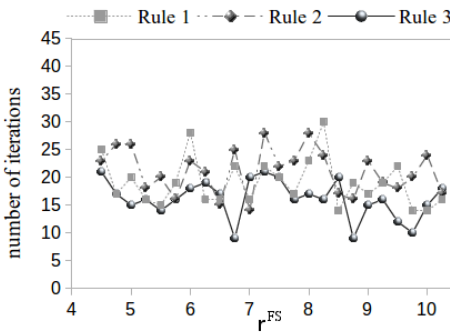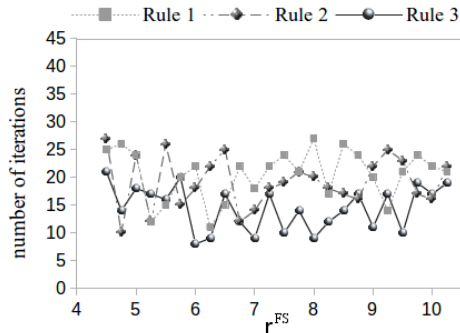
(a) 3x3 points.

(b) 4x4 points.

(c) 5x5 points.

(d) 7x7 points.

(e) 9x9 points.

Figure 8: Comparing the number of iterations for the different number of Gauss points and r^{FS} values.

References

Atluri, S. N.; Zhu, T. (1998):   A new meshless local Petrov-Galerkin (MLPG) approach in computational mechanics. *Comput. Mech.*, vol. 22, pp. 117–127.

Atluri, S. N.; Zhu, T. (2000):   The meshless local Petrov-Galerkin (MLPG) approach for solving problems in elastostatics. *Computational Mechanics*, vol. 25, pp. 169–179.

Castor, G. S.; Telles, J. C. F. (2000):   The 3-D bem implementation of a numerical green's function for fracture mechanics applications.   *International Journal for Numerical Methods in Engineering*, vol. 48, no. 8, pp. 1199–1214.

Ching, H.-K.; Batra, R. C. (2001):   Determination of crack tip field in linear elastostatics by the meshless local Petrov-Galerkin (MLPG) method.   *Computer Modelling in Engineering and Sciences*, vol. 2, pp. 273–289.

De, S.; Bathe, K.-J. (2001):   The method of finite spheres with improved numerical integration. *Computers & Structures*, vol. 79, pp. 2183–2196.

Fontes Jr., E. F.; Santiago, J. A. F.; Telles, J. C. F. (2013):   On a regularized method of fundamental solutions coupled with the numerical Green's function procedure to solve embedded crack problems. *Eng Anal Boundary Elem*, vol. 37, pp. 1–7.

Godinho, L.; Soares Jr., D. (2013):   Frequency domain analysis of interacting acoustic-elastodynamic models taking into account optimized iterative coupling of different numerical methods. *Eng Anal Boundary Elem*, vol. 32, pp. 1074–1088.

Gu, Y. T.; Zhang, L. C. (2008):   Coupling of the meshfree and finite element methods for determination of the crack tip fields. *Engineering fracture mechanics*, vol. 75, pp. 986–1004.

Guimaraes, S.; Telles, J. C. F. (2000):   General Application of Numerical Green's Functions for SIF Computations With Boundary Elements. *Computer Modelling in Engineering and Sciences*, vol. 1, pp. 131–139.

Han, Z. D.; Atluri, S. N. (2002):   SGBEM (for cracked local subdomain)-FEM (for uncracked global structure) alternating method for analyzing 3D surface cracks and their fatigue-growth. *Computer Modelling in Engineering and Sciences*, vol. 3, no. 6, pp. 699–716.

Jayan, S.; Nagaraja, K. V. (2011): Generalized Gaussian quadrature rules over two-dimensional regions with linear sides. *Applied mathematics and computation*, vol. 217, pp. 5612–5621.

Kupradze, V. D.; Aleksidze, M. A. (1964): The method of functional equations for the approximate solution of certain boundary value problems. *U.S.S.R. Computational Mathematics and Mathematical Phisics*, vol. 4, pp. 82–126.

Lancaster, P.; Salkauskas, K. (1981): Surfaces generated by moving least squares methods. *Mathematics of Computation*, vol. 37, pp. 141–158.

Lin, C. C.; Lawton, E. C.; Caliendo, J. A.; Anderson, L. R. (1996): An iterative finite element-boundary element algorithm. *Computers & Structures*, vol. 59, pp. 899–909.

Ma, J.; Rokhlin, V.; Wandzura, S. (1996): Generalized Gaussian Quadrature Rules for Systems of Arbitrary Functions. *SIAM Journal on Numerical Analysis*, vol. 33, no. 3, pp. 971–996.

Mazzia, A.; Ferronato, M.; Pini, G.; Gambolati, G. (2007): A comparison of numerical integration rules for the meshless local Petrov-Galerkin method. *Numer Algor.*, vol. 45, pp. 61–74.

Mazzia, A.; Pini, G. (2010): Product Gauss quadrature rules vs. cubature rules in the meshless local Petrov-Galerkin method. *Journal of complexity*, vol. 26, pp. 82–101.

Miers, L. S.; Telles, J. C. F. (2006): On the NGF Procedure for LBIE Elastostatic Fracture Mechanics. *Computer Modelling in Engineering and Sciences*, vol. 14, no. 3, pp. 161–169.

Nguyen, V. P.; Rabczuk, T.; Bordas, S.; Duflot, M. (2008): Meshless methods: A review and computer implementation aspects. *Mathematics and Computers in Simulation*, vol. 79, pp. 763–813.

Pecher, R. (2006): Efficient cubature formulae for MLPG and related methods. *Int. J. Numer. Methods Eng.*, vol. 65, pp. 566–593.

Pierce, W. H. (1957): Numerical integration over planar annulus. *J. Soc. Ind. Appl. Math.*, vol. 5, no. 2, pp. 66–73.

Snyder, M. D.; Cruse, T. A. (1975): Boundary integral equation analysis of cracked anisotropic plates. *International Journal of Fracture*, vol. 11, pp. 315–328.

Telles, J. C. F.; Castor, G. S.; Guimaraes, S. (1995): A numerical Green's function approach for boundary elements applied to fracture mechanics. *International Journal for Numerical Methods in Engineering*, vol. 38, pp. 3259–3274.

Thomas, G. B.; Finney, R. L. (1996):   *Calculus and Analytic Geometry.* Addison-Wesley.